Epitaxial graphene on 6H-SiC and Li intercalation

Chariya Virojanadara, Somsakul Watcharinyanon, A A Zakharov and Leif I Johansson

Original Publication:

Chariya Virojanadara, Somsakul Watcharinyanon, A A Zakharov and Leif I Johansson, Epitaxial graphene on 6H-SiC and Li intercalation, 2010, PHYSICAL REVIEW B, (82), 20, 205402.
http://dx.doi.org/10.1103/PhysRevB.82.205402

PHYSICAL REVIEW B **82**, 205402 (2010)

Epitaxial graphene on 6*H*-SiC and Li intercalation

C. Virojanadara,[1] S. Watcharinyanon,[1] A. A. Zakharov,[2] and L. I. Johansson[1]
[1]*Department of Physics, Chemistry, and Biology, Linköping University, S-581 83 Linköping, Sweden*
[2]*Maxlab, Lund University, S-22100 Lund, Sweden*
(Received 14 July 2010; revised manuscript received 30 September 2010; published 4 November 2010)

The influence of lithium (Li) exposures on monolayer graphene grown on the silicon-terminated SiC(0001) surface is investigated using low-energy electron microscopy, photoelectron spectroscopy, and micro-low-energy electron diffraction. After Li deposition, islands or Li droplets are observed on the surface, and are found to coalesce together with time. Formation of a dipole layer at the interface, interpreted to originate from Li-Si bonding, is observed directly after Li deposition, and manifested by a 2 eV shift of the C 1*s* and Si 2*p* bulk SiC peaks. This indicates that Li atoms penetrate through the graphene and carbon buffer layer directly after deposition at room temperature since three π bands are then moreover observed at the K point, instead of the single π band for monolayer graphene. The existence of three π bands is interpreted as a mixture of bilayer and monolayer graphene plus a difference in doping levels due to an uneven distribution of Li atoms. Li gives rise to electron doping of the graphene and results in a lowering of the Dirac point. After annealing to a few hundred degrees Celsius, a more even Li distribution and intercalation is obtained since then two distinct π bands appear at the K point.

DOI: 10.1103/PhysRevB.82.205402 PACS number(s): 73.22.Pr, 73.22.−f

I. INTRODUCTION

Graphene, a single sheet of graphite, is known to be one of the most promising materials for C-based electronics. This is because it has high mobility of charge carriers and ballistic transport over long distances.[1] However, the existence of a carbon buffer layer is known for the epitaxial graphene prepared on SiC(0001) substrates. This layer has no graphitic electronic properties, acts as a buffer layer and allows the next carbon layer to behave electronically like an isolated graphene sheet. This buffer layer exhibits however a large band gap and a Fermi level pinned by a state related to the dangling bonds on Si atoms in the SiC bilayer closest to the buffer layer.[1] This layer is regarded as a major obstacle for the development of future electronic devices from graphene grown on SiC(0001). Our earlier work[2] has successfully demonstrated that the buffer layer underneath a single-sheet graphene can be eliminated or converted to become a second graphene layer by atomic hydrogen exposures at an elevated substrate temperature. To fully passivate the Si dangling bonds at the interface by hydrogen is, however, not a simple task. It has moreover been claimed[3] that hydrogen atoms can attach to each site of the graphene lattice and change the hybridization of carbon atoms from sp^2 into sp^3 and thus remove the conducting π bands and open up an energy gap. Yang[4] claimed that just like hydrogen, lithium is a good candidate for reacting with graphene by turning the original sp^2 hybridization of the carbon atoms into that of sp^3. Additionally, the doping of single wall carbon nanotubes by Li and K is known to enhance the conductivity and hydrogen storage capacity.[5] Only theoretical studies of the adsorption of lithium on graphene[4,6–8] have to our knowledge so far been published and therefore we pursued the detailed experimental investigation reported below.

II. EXPERIMENT

Our graphene was grown on nominally on-axis 6*H*-SiC(0001) substrates with a misorientation error within 0.06°. The wafers were production grade *n*-type from SiCrystal with chemical and mechanical polishing on the Si face. The growth of homogeneous monolayer graphene on the 6*H*-SiC(0001) substrate was performed by heating the sample *in situ* at a temperature of 1300 °C for a few minutes at a base pressure of approximately 10^{-10} mbar. The sample was mounted in a special way, with the Si face facing down toward the sample holder while heating to increase the Si vapor pressure above the surface. The quality of the as-grown graphene prepared this way is demonstrated in the low-energy electron microscopy (LEEM) image in Fig. 1(a). The morphology, electronic structure, and thickness of the graphene layers grown were investigated using LEEM, photoelectron spectroscopy (PES), and micro-low-energy electron diffraction (μ-LEED) on beamline I311 at MAX laboratory. This beamline is equipped with a modified SX-700 monochromator, which provides light for two end stations. The first station is built around a large hemispherical Scienta electron analyzer which operates at a base pressure of about 1×10^{-10} mbar. A total-energy resolution determined by the operating parameter used, of <10 to 100 meV at a photon energy from 33 to 450 eV and of <300 meV at a photon energy from 600 to 750 eV were selected in the high-resolution studies of the C 1*s*, Si 2*p*, and Li 1*s* core levels and the valence bands reported below. The second station is equipped with a spectroscopic photoemission LEEM (SPELEEM) instrument. This microscope has a spatial resolution better than 10 nm in the LEEM mode. Additional angle-resolved photoemission spectroscopy (ARPES) was performed at beamline I4 at the same facility. This beamline is equipped with a spherical grating monochromator and PHOIBOS 100 two-dimensional (2D) Specs energy analyzer. The low angular dispersion lens mode was selected which provided an acceptant angle of ±7°. The samples were kept at room temperature and exposed to a Li flux from a SAES getter source for a few minutes. The evolution of the Li

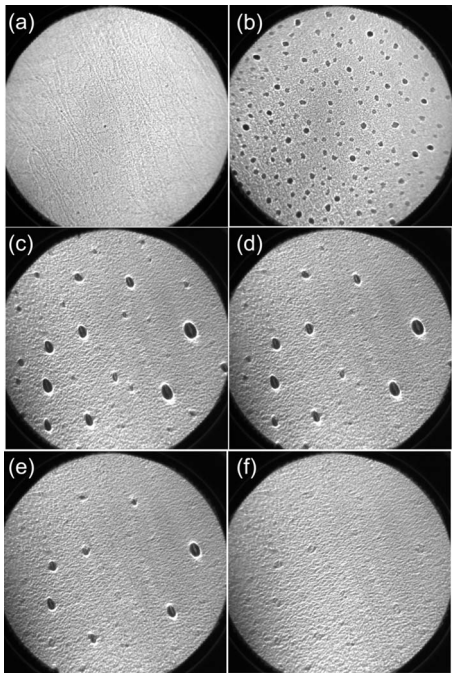

FIG. 1. (a) LEEM image of a monolayer graphene grown on SiC(0001); the field of view (FOV) is 50 μm and the electron energy is $E_{vac}-0.5$ eV. (b) LEEM image illustrating the graphene surface after Li deposition; the same FOV and the electron energy $E_{vac}-1.7$ eV is used in this case. (c)–(f) LEEM images recorded after annealing the sample to 290 °C, 310 °C, 320 °C, and 330 °C, respectively; the electron energy is $E_{vac}-1.7$ eV and the FOV is 25 μm.

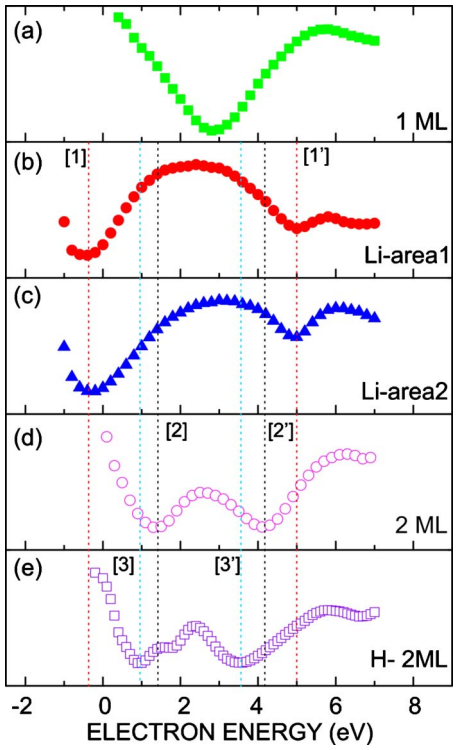

FIG. 2. (Color online) Electron reflectivity curve recorded (a) from monolayer graphene before Li deposition, (b) and (c) from two different areas in Fig. 1(b) after lithium deposition. From area1—bright gray area and area2—black island, respectively. The electron reflectivity curve (d) is from a bilayer *ex situ* grown sample (Ref. 10) and (e) from a bilayer sample obtained after hydrogen intercalation (Ref. 2).

intercalation with annealing temperature was investigated live in front of the objective lens in the SPELEEM station.

III. RESULTS AND DISCUSSIONS

Figure 1 displays LEEM images of an *in situ* prepared graphene layer before, Fig. 1(a), and after, Fig. 1(b), Li deposition and also after annealing sequences from 290–330 °C [Figs. 1(c)–1(f)]. Small islands were observed directly after Li deposition at room temperature, which were found to coalesce with time and also with annealing. These islands moreover reduced upon annealing as illustrated in Figs. 1(c)–1(f). At a temperature of around 330 °C, the islands essentially disappeared and could no longer be observed by LEEM. One may think that Li starts to leave the sample already at this low annealing temperature since graphene is known to function as a nanonet material. Even H, the smallest atom cannot pass through the graphene at room temperature. The core-level spectra presented and discussed below show, however, that this is not the case.

The electron reflectivity curves (*I-V*) collected before and after Li deposition show significant differences. In Fig. 2(a), one minimum (dip) is observed at an energy of around 3 eV. This represents monolayer graphene before deposition and agrees well with earlier observations.[9–11] The *I-V* spectra collected after Li deposition are plotted in Figs. 2(b) and 2(c) and correspond to two different selected areas, i.e., the bright gray area (area 1) and the dark island (area 2), respectively. Interestingly, two minima are now observed at energies of around −0.4 and 5 eV, which suggests the presence of two instead of one graphene layer. Moreover the shift of the reflectivity threshold to lower electron energy after Li deposition indicates a decrease in the work function of the sample.[12] It should also be noted that the spectra in Figs. 2(b) and 2(c) appear significantly different compared to those displayed in Figs. 2(d) and 2(e). The *I-V* spectrum in Fig. 2(d) was collected from an *ex situ* grown bilayer graphene[10] sample and the spectrum in the Fig. 2(e) from a hydrogen-intercalated[2] bilayer sample. Slightly shifted minima were observed for the hydrogen-intercalated sample but the separation between the minima remained similar as for the *ex situ* grown bilayer graphene sample, i.e., cf. Figs. 2(d) and 2(e). This is, however, not the case after Li deposition where a larger separation between the two minima is clearly observed. We suggest this to be caused by Li atoms penetrating through, and in between, the graphene and buffer layer and into the interface and thereby inducing changes in the electron diffraction path. A lowering of the work function of the sample was also clearly observed by LEEM.

The changes induced in the C 1*s* and Si 2*p* core-level spectra after Li deposition and consecutive anneals were investigated, as illustrated in Figs. 3 and 4, respectively. A set of C 1*s* spectra, collected using a photon energy of 450 eV, is shown in Fig. 3(a). The C 1*s* spectrum of monolayer

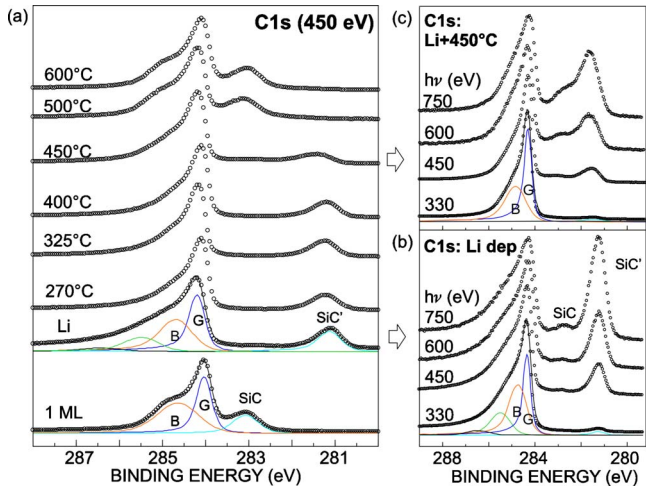

FIG. 3. (Color online) C 1*s* core level spectra collected (a) at 450 eV photon energy from the monolayer graphene sample, before and after lithium deposition and annealing from 270 to 600 °C, (b) at different photon energies after Li deposition and (c) after annealing to 450 °C.

graphene on SiC(0001) contains three components,[10] i.e., bulk SiC, graphene (G), and carbon interface layer (B), the so-called buffer layer, as seen in the bottom curve. After Li deposition, the bulk SiC component (now labeled SiC′) is observed to shift by about 2 eV to lower binding energy and a broad shoulder is detected on the higher binding energy side of the buffer layer peak. The shift is interpreted to indicate formation of a dipole layer at the graphene-SiC interface, i.e., that Li atoms have penetrated into the interface region and interacts with the SiC substrate. Also the appearance of the shoulder is suggested to arise from these interactions, i.e., changes in the coulomb charge density in the interface region. After annealing from 270 to 450 °C the intensity of this shoulder and the buffer layer peak are reduced while on the other hand, the graphene/SiC relative intensity ratio (G/SiC′ peak ratio) has increased. These intensity ratios obtained after Li deposition and intercalation are somewhat different compared to those observed after hydrogenation.[2] The B/SiC intensity ratio clearly decreased and the G/SiC ratio increased by about a factor of 2 after hydrogenation. In the case of Li intercalation, the same trend but smaller changes are observed. This suggests that Li atoms are not as efficient as H atoms in decoupling the carbon buffer layer from the substrate. Some interaction remains, which do not allow the buffer layer to behave like a second quasi free standing graphene layer as in the hydrogen case. The C 1*s* spectra recorded at different photon energies (i.e., from very surface sensitive (330 eV) to bulk sensitive (750 eV)) after Li deposition and after annealing at 450 °C are shown in Figs. 3(b) and 3(c), respectively. The intensity of the shifted bulk (SiC′) component does increase with increasing photon energy, which shows that this component originates from the interface and bulk region underneath the graphene and buffer layer. These spectra moreover show clearly that most of the interface area contains Li, resulting in the shifted bulk component (SiC′). Only a very weak signal from the unshifted bulk (SiC) component is observed after Li deposition but after annealing at 450 °C it becomes more visible. This is interpreted to be due to that Li atoms have started to leave the interface region at this temperature.

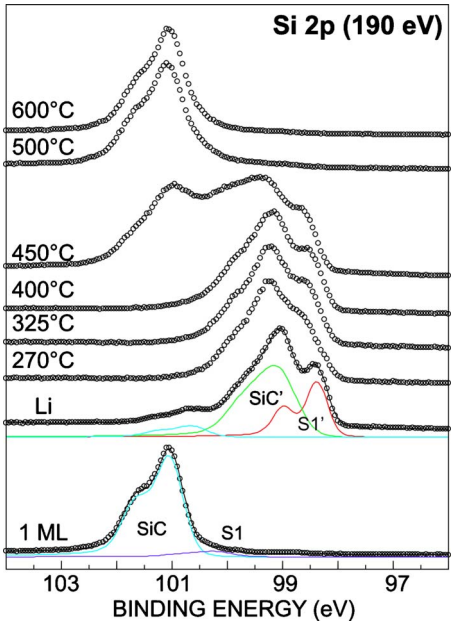

FIG. 4. (Color online) Si 2*p* spectra collected at 190 eV photon energy from the monolayer graphene sample, before and after Li deposition and annealing from 270 to 600 °C.

Similar effects were also observed in recorded Si 2*p* spectra, as illustrated in Fig. 4 using a photon energy of 190 eV. The spectrum before Li deposition contains mainly contribution from the bulk SiC substrate. However, a small shifted component interpreted to originate from the uppermost Si-C bilayer, is also observed and labeled S1. After deposition, both the SiC and S1 components (now labeled SiC′ and S1′, respectively) are found to be shifted about 2 eV to lower binding energy. This is consistent with the shift observed in the C 1*s* spectrum, and indicates formation of a dipole layer at the graphene-SiC interface. Part of the shift can actually be due to a change in the pinning of the Fermi level in the SiC substrate[13] when Li is present at the interface. A flatband condition is nearly obtained for the graphitized *n*-doped SiC(0001) surface while an appreciable band bending may occur after adsorption of a metal that can pin the Fermi level closer to the middle of the band gap. In the photoemission measurements, we cannot disentangle contributions from a Li-induced band bending and a Li interface dipole layer but merely say that the sum of these effects provides a shift of approximately 2.0 eV in the C 1*s* and Si 2*p* levels of the SiC substrate. It deserves to be noted that the Gaussian width obtained in the fit of the Si 2*p* doublet was, respectively 0.6 eV, 0.7 eV, and 0.4 eV for the SiC, SiC′, and S1′ components. The S1 component also becomes more intense and sharper after Li deposition, which show that there are interactions between Si and Li near the interface region. The intensity of the S1 component was found to decrease with increasing photon energy confirming that the S1 peak originates from Si atoms located closer to the surface than those giving rise to the SiC′ bulk component. After annealing at 450 °C, the Si 2*p* spectrum has become twice as broad as

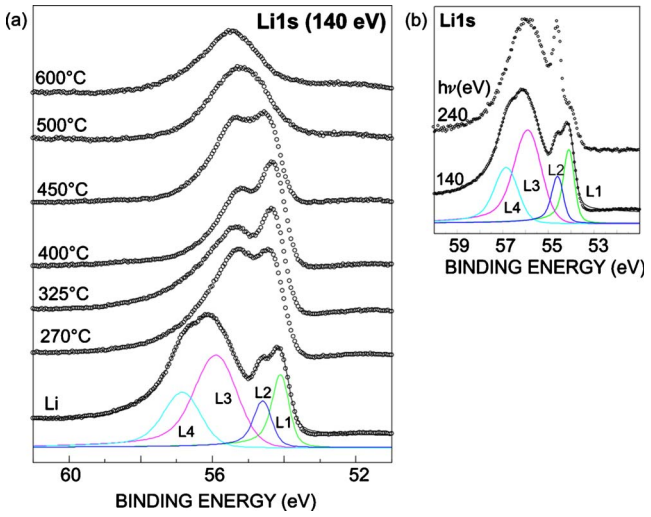

FIG. 5. (Color online) Li 1*s* spectra collected (a) at 140 eV photon energy after deposition and annealing from 270 to 600 °C, (b) at two different photon energies after Li deposition.

before. This we interpret to be due to that part of Li atoms have started to move away from the interface region, which affects the dipole layer formed. We suggest that a mixture of intercalated and nonintercalated areas are now observed by photoemission. This is consistent with the larger SiC/SiC′ intensity ratio seen in the C 1*s* spectrum in Fig. 3(c) than in Fig. 3(b). After heating at 500 °C both the Si 2*p* and C 1*s* spectra are essentially back to the shape they had before the Li deposition.

Li 1*s* spectra recorded from the same deposition and annealing cycle at a photon energy of 140 eV are shown in Fig. 5(a). Directly after Li deposition, four components, labeled L1–L4, were required to produce good fits to the experimental data. The L1 component is, as illustrated in Fig. 5(b), surface related and it was found to decrease in intensity directly upon heating. X-ray photoemission electron microscope (XPEEM) measurements demonstrated that the L1 component signal did include also the dark spots seen on the LEEM image in Fig. 1(b). This was done by collecting XPEEM images from the Li 1*s* core level at the binding energy of the L1 component and then these dark spots instead appeared slightly brighter than the other areas. No such contrast could be observed in the XPEEM images recorded using any of the other components. This may be due to a few reasons; either the component is distributed homogeneously over the surface or the intensity variation is too low to detect since it may be located deep down close to the interface. The L1 component is suggested to correspond to the ordered Li that partially occupies the graphene π bonds on the surface as illustrated by the μ-LEED patterns in Fig. 6. A well-ordered (1×1) graphene pattern with the additional $6\sqrt{3}\times6\sqrt{3}-R30°$ spots from the buffer layer is normally observed for monolayer graphene, as displayed in Fig. 6(a). Directly after Li deposition, the $6\sqrt{3}$ spots can no longer be observed but instead a new reconstructed pattern similar to $\sqrt{3}\times\sqrt{3}-R30°$ could be detected as shown in Fig. 6(b). This observation agrees well with the predictions of an earlier theoretical study.[7] This may imply that Li atoms have occupied 1/3 of the π bonds on the graphene surface, giving rise to this new reconstructed LEED pattern. However, this pattern fainted away directly upon heating and then mainly the graphene spots could be observed, as illustrated in Fig. 6(c). In the Li 1*s* spectrum significant changes were observed after annealing since then mainly L2, L3 and L4 could be observed. Among these the L2 seems to be the most bulk sensitive component as illustrated in Fig. 5(b) and therefore it is suggested to correspond to Li atoms at the interface that bond to Si atoms in the topmost Si-C bilayer, as reflected by the S1 component observed in Si 2*p* spectra in Fig. 4. For the L3 and the L4 components, we suggest that they correspond to Li atoms interacting with the buffer layer and Li atoms in between the graphene sheet and the buffer layer, respectively. The intensities of the L3 and the L4 components show similar variations with photon energy and therefore they should originate from a similar probing depth. However, the intensity of the L4 component goes down with increasing annealing temperature and can no longer be detected after annealing at 400 °C while the L3 remains throughout the heating cycle. In order to confirm our interpretation concerning the origin of the different components, Li was also deposited on a clean and well-ordered SiC(0001)-$\sqrt{3}\times\sqrt{3}R30°$ surface prepared by *in situ* heating. A similar amount of Li was deposited on this sample, kept at room temperature. A simple layer attenuation model was utilized to estimate the amount of Li deposited and gave in this case, and also for the case presented in Figs. 3–5 after heating at 270 °C, a layer thickness of about 2–3 Å, which roughly corresponds to one ML of Li. Only the L2 and L3 components could then be detected in the Li 1*s* spectrum. It should be noted that this $\sqrt{3}$ reconstructed SiC surface prepared by *in situ* heating contains Si adatoms, a Si-terminated Si-C bilayer but also some carbon clusters (starting phase for the carbon buffer layer).[13] Therefore, on this surface Li atoms can only interact with Si atoms in the outermost layers and the carbon clusters and result in, respectively, the L2 and L3 components in the Li 1*s* spectrum.

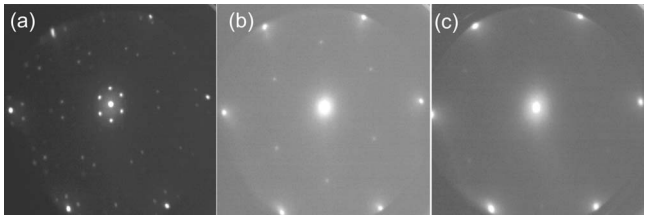

FIG. 6. μ-LEED images collected at $E_{kin}=40$ eV from (a) monolayer graphene, (b) after Li deposition, and (c) after annealing to 325 °C.

The ARPES results obtained from this sample also supports the point of view that the Li atoms have penetrated the graphene and buffer layer and have intercalated as demonstrated in Fig. 7. Before Li deposition, the monolayer graphene sample showed a single π band and a Dirac point at approximately 0.4 eV below the Fermi level as displayed in Fig. 7(a). Of particular interest is that after Li deposition, three π bands are clearly observed, Fig. 7(b). It is, however, impossible to create trilayer graphene from only a single sheet of graphene plus a buffer layer. Therefore we suggest

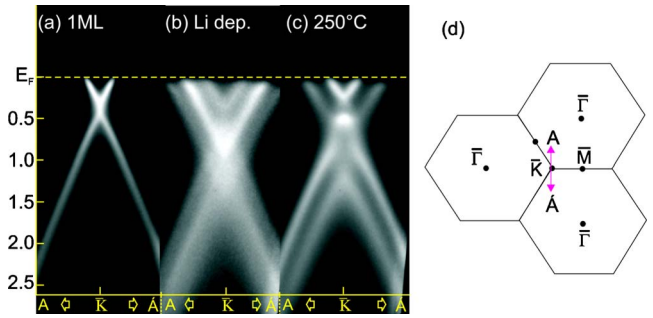

FIG. 7. (Color online) The π band around the K point recorded from (a) monolayer graphene, (b) after Li deposition, and (c) after annealing at 250 °C. (d) Schematic drawing of the 2D Brillouin zone of graphene and the direction of scan.

that the three π bands represent a mixture of bilayer and monolayer graphene but with different amount of doping, i.e., an unevenly distribution of Li in the surface region [as indicated by Fig. 1(b)]. After heating the sample from 250–450 °C only two sharp π bands are observed suggesting that a more even intercalation and distribution of Li has been accomplished, as indicated by Figs. 1(f) and 6(c). In addition, the Dirac point energy (E_D) is after the deposition shifted toward higher binding energy by about 0.25–0.5 eV, depending on the Li coverage. This indicates, as expected, electron doping of the graphene instead of the hole doping observed upon hydrogenation. Also the band-structure data provide some support for the theoretical model[6,7] of Li adsorption in the hollow sites (C_6Li) on graphene producing a $\sqrt{3}\times\sqrt{3}R30°$ structure but not the model of Li adsorption in top positions on both sides of graphene producing a (1×1) adsorption structure and a rippled graphene layer. The calculated band structure[7] of C_6Li shows—a shift of the Dirac point by about 1.5 eV away from the Fermi level—an opening of a band gap of 0.4 eV at the Dirac point—a lifting of the degeneracy of the bands in graphene (C_{6*}) so two or eventually three bands should be observable for C_6Li between the Dirac point and the Fermi level and—a very similar dispersion of the bands around K point in the Brillouin zone for C_{6*} and C_6Li. The other adsorption model[4,8] also shift the Dirac point away from the Fermi level but the energy bands located between the Dirac point and the Fermi level obtain quite different dispersions around K point compared to the bands in graphene. Our experimental band structure after Li deposition do not agree at all with those[4,8] calculated results but show some resemblance with the band structure[7] calculated for C_6Li. It should be noted that Li deposited on monolayer graphene may possibly give rise to plasmarons, i.e., a coupling between electrons and plasmons, similar to the recent observation[14] for potassium. In order to try to conclude if this is the case also for Li, additional experimental and theoretical work is required.

Normal emission valence-band spectra collected using a photon energy of 33 eV and under the same conditions as the core levels presented above are shown in Fig. 8. The valence-band spectrum is seen to contain two main components located at about 5 and 8.5 eV below the Fermi level and originating, respectively, from a σ and π band. After Li deposition the σ component, which represents the in plane

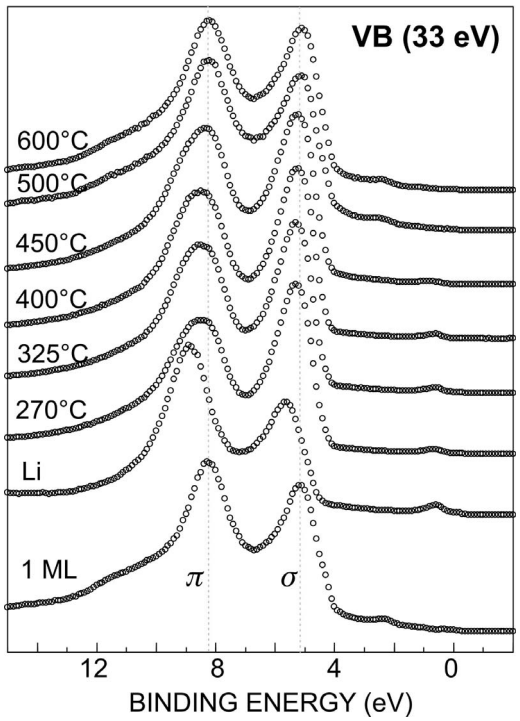

FIG. 8. Valence-band spectra recorded at normal emission, at a photon energy of 33 eV, before and after Li deposition and annealing from 270 to 600 °C.

sp^2 bonding, is observed to decrease in intensity and shift to higher binding energy. The former is an indication that the C-C sp^2 bonds are broken, i.e., disorder is induced, by the Li deposition. The latter is an indication of charge transfer, of n-type doping, and a lowering of the work function after Li deposition. However the σ component has regained strength directly after the heating and the spectra have shifted back to the similar value again. These observations agree very well with the appearance of diffuse π bands observed in Fig. 7(b) after Li deposition.

IV. SUMMARY

We have demonstrated an intercalation process of Li at room temperature in monolayer graphene samples prepared epitaxially on SiC(0001). Our results show that Li atoms penetrate through the graphene as well as the carbon buffer layer and intercalate at the interface between SiC and the buffer layer. The process starts immediately after deposition. Some of the Li atoms do, however, interact with the buffer layer as well as with the graphene sheet creating defects that disappear upon annealing. The Li atoms are suggested to bond to the Si atoms in the uppermost Si-C bilayer at the interface and to create a dipole layer in the interface region that induces an approximately 2 eV shift of the bulk SiC core level. These Li atoms do at the same time also lift up part of the buffer layer from the substrate and transform it into a second graphene layer. After deposition at room temperature

these graphene layers appear, however, disturbed by an uneven distribution of Li atoms since three π bands then are observed at the K point. After annealing to a few hundred degree Celsius a more even Li distribution and intercalation is obtained since then two distinct π bands appear at the K point. Li gives rise to electron doping of the graphene and results in a lowering of the Dirac point energy (E_D) by 0.25–0.5 eV depending on Li coverage. The Li intercalated samples were found to be stable up to a temperature of around 450 °C.

ACKNOWLEDGMENTS

Support from the Swedish National Energy Administration is gratefully acknowledged.

[1] C. Berger, X. Wu, P. N. First, E. H. Conrad, X. Li, M. Sprinkle, J. Hass, F. Varchon, L. Magaud, M. L. Sadowski, M. Potemski, G. Martinez, and W. A. de Heer, Adv. Solid State Phys. **47**, 145 (2008), and reference therein.

[2] C. Virojanadara, A. A. Zakharov, R. Yakimova, and L. I. Johansson, Surf. Sci. **604**, L4 (2010).

[3] D. C. Elias, R. R. Nair, T. M. G. Mohiuddin, S. V. Morozov, P. Blake, M. P. Halsall, A. C. Ferrari, D. W. Boukhvalov, M. I. Katsnelson, A. K. Geim, and K. S. Novoselov, Science **323**, 610 (2009).

[4] C.-K. Yang, Appl. Phys. Lett. **94**, 163115 (2009).

[5] P. Chen, X. Wu, J. Lin, and K. L. Tan, Science **285**, 91 (1999).

[6] M. Khantha, N. A. Cordero, L. M. Molina, J. A. Alonso, and L. A. Girifalco, Phys. Rev. B **70**, 125422 (2004).

[7] M. Farjam and H. Rafii-Tabar, Phys. Rev. B **79**, 045417 (2009).

[8] P. V. C. Medeiros, F. de Brito Mota, A. J. S. Mascarenhas, and C. M. C. de Castilho, Nanotechnology **21**, 115701 (2010).

[9] H. Hibino, H. Kageshima, F. Maeda, M. Nagase, Y. Kobayashi, and H. Yamaguchi, Phys. Rev. B **77**, 075413 (2008).

[10] C. Virojanadara, M. Syväjarvi, R. Yakimova, L. I. Johansson, A. A. Zakharov, and T. Balasubramanian, Phys. Rev. B **78**, 245403 (2008).

[11] C. Virojanadara, R. Yakimova, A. A. Zakharov, and L. I. Johansson, J. Phys. D: Appl. Phys. **43**, 374010 (2010).

[12] H. Hibino, H. Kageshima, M. Kotsugi, F. Maeda, F.-Z. Guo, and Y. Watanabe, Phys. Rev. B **79**, 125437 (2009).

[13] L. I. Johansson, F. Owman, and P. Mårtensson, Phys. Rev. B **53**, 13793 (1996).

[14] A. Bostwick, F. Speck, Th. Seyller, K. Horn, M. Polini, R. Asgari, A. H. MacDonald, and E. Rotenberg, Science **328**, 999 (2010).